NEOPLASIA
www.neoplasia.com

Volume 20 Number 9 September 2018 pp. 951–963 951

Downregulation of Rap1Gap: A Switch from DCIS to Invasive Breast Carcinoma *via* ERK/MAPK Activation[1]

Seema Shah[*], Ethan J. Brock[*], Ryan M. Jackson[†], Kyungmin Ji[†], Julie L. Boerner[*], Bonnie F. Sloane[*,†] and Raymond R. Mattingly[*,†]

[*]Department of Oncology, Wayne State University School of Medicine, Detroit, MI, USA; [†]Department of Pharmacology, Wayne State University School of Medicine, Detroit, MI, USA

Abstract

Diagnosis of breast ductal carcinoma *in situ* (DCIS) presents a challenge since we cannot yet distinguish those cases that would remain indolent and not require aggressive treatment from cases that may progress to invasive ductal cancer (IDC). The purpose of this study is to determine the role of Rap1Gap, a GTPase activating protein, in the progression from DCIS to IDC. Immunohistochemistry (IHC) analysis of samples from breast cancer patients shows an increase in Rap1Gap expression in DCIS compared to normal breast tissue and IDCs. In order to study the mechanisms of malignant progression, we employed an *in vitro* three-dimensional (3D) model that more accurately recapitulates both structural and functional cues of breast tissue. Immunoblotting results show that Rap1Gap levels in MCF10.Ca1D cells (a model of invasive carcinoma) are reduced compared to those in MCF10.DCIS (a model of DCIS). Retroviral silencing of Rap1Gap in MCF10.DCIS cells activated extracellular regulated kinase (ERK) mitogen-activated protein kinase (MAPK), induced extensive cytoskeletal reorganization and acquisition of mesenchymal phenotype, and enhanced invasion. Enforced reexpression of Rap1Gap in MCF10.DCIS-Rap1GapshRNA cells reduced Rap1 activity and reversed the mesenchymal phenotype. Similarly, introduction of dominant negative Rap1A mutant (Rap1A-N17) in DCIS-Rap1Gap shRNA cells caused a reversion to nonmalignant phenotype. Conversely, expression of constitutively active Rap1A mutant (Rap1A-V12) in noninvasive MCF10.DCIS cells led to phenotypic changes that were reminiscent of Rap1Gap knockdown. Thus, reduction of Rap1Gap in DCIS is a potential switch for progression to an invasive phenotype. The Graphical Abstract summarizes these findings.

Neoplasia (2018) 20, 951–963

Abbreviations: DA, dominant active; DN, dominant negative; DCIS, ductal carcinoma *in situ*; ECM, extracellular matrix; EMT, epithelial to mesenchymal transition; ERK, extracellular-signal regulated kinase; ER, estrogen receptor; GAP, GTPase activating protein; GFP, green fluorescent protein; GTP, guanosine triphosphate; HER2, human epidermal growth factor receptor-2; IDC, invasive ductal cancer; IHC, immunohistochemistry; LOH, loss of heterozygosity; MAPK, mitogen-activated protein kinase; rBM, reconstituted basement membrane; PR, progesterone receptor; TN, triple negative; 3D, three-dimensional.

Address all correspondence to: Raymond R. Mattingly, Department of Pharmacology Wayne State University School of Medicine, 540 E. Canfield Ave., Detroit, MI 48201.
E-mail: r.mattingly@wayne.edu

[1] This work was partially supported by R01 CA131990, the Molecular Therapeutics program of the Karmanos Cancer Institute, and the Wayne State University Office of the Vice-President for Research, and aided by the Imaging and Cytometry and Biobanking and Correlative Sciences core facilities, which are supported in part by P30 CA022453. E. J. B. was supported by T32 CA009531 and F31 CA213807. R. M. J. was supported by R25 GM058905. K. J. was supported by R21 CA175931, U54CA193489, and the PHC Research Stimulation Fund.
Received 15 December 2017; Revised 6 July 2018; Accepted 12 July 2018

1476-5586
https://doi.org/10.1016/j.neo.2018.07.002

Graphical abstract

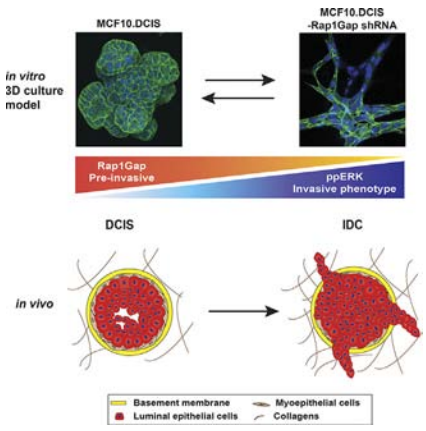

Down-regulation of Rap1Gap: A switch from DCIS to IDC via ERK/MAPK activation. The confocal immunofluorescence images (collapsed z-stacks; 40x magnification) are of *in vitro* 3D culture models of MCF10.DCIS. Green and blue represent F-actin cytoskeleton and nuclei, respectively. When Rap1Gap is reduced by shRNA, ERK is activated and there is acquisition of an invasive phenotype. Conversely, when Rap1Gap is re-expressed in the DCIS Rap1Gap shRNA cells, there is reversion to a pre-invasive phenotype. The *in vitro* 3D culture model recapitulates findings from DCIS and IDC patient samples.

Neoplasia (2018) 20, 951–963

Introduction

Mortality from breast cancer has declined for the past 2 decades, and this decline [1] might be due to introduction of screening programs in the 1980s, resulting in earlier diagnosis and intervention [2]. Ductal carcinoma *in situ* (DCIS) accounts for 15%-25% of newly diagnosed breast cancer cases in the United States [3]. Until 1980, DCIS represented less than 1% of breast cancer [4]. The apparent incidence has increased, in part, due to the rise in use of mammography screens and improved imaging technologies [5]. It is still unclear which DCIS lesions will become invasive or will remain indolent during a woman's lifetime [6,7]. As a result, many women with low-risk DCIS are offered treatment that may not benefit them [8]. We thus need to better define the factors that determine progression from DCIS to invasive ductal carcinoma of the breast (IDC). Molecular profiling has identified the same cancer subtypes in DCIS that are found in IDC [9,10], and thus it is reasonable to propose that the invasive progression may be induced more by loss of suppressive activities than by the gain of additional oncogenic drivers [11].

Using next-generation sequencing, we found a consensus group of 63 upregulated genes in human DCIS cells grown in three-dimensional (3D) cultures relative to control nontransformed immortalized human mammary epithelial cells [7]. Rap1Gap, one of those 63 upregulated genes, encodes a negative regulator of the small GTPase Rap1. Rap1 is a key determinant in mammary acinar structure [12] and is overexpressed in breast IDC and in *in situ* lesions that are adjacent to invasive disease [13]. Although a role for the loss of Rap1Gap in breast cancer progression has not previously been defined, there is strong evidence for its tumor-suppressive activities in other malignancies (including melanoma and thyroid, renal, pancreatic, and oropharyngeal cancers) through inhibition of proliferation, migration [14–16], invasion [17,18], and motility [19].

In order to investigate the potential tumor suppressive role of Rap1Gap in DCIS progression to IDC, we employed the MCF10 progression series, which includes MCF10.DCIS and MCF10.Ca1D cells, to model human DCIS and IDC, respectively. The MCF10 series is a group of cell lines derived from MCF10A cells (which were established by the spontaneous immortalization of human breast epithelial cells originally isolated from a patient) [20]. The second member of the series, MCF10.NeoT, was generated after transforming MCF10A *via* transfection with mutated T24 *H-ras*. When injected into immunodeficient nude mice, the MCF10.NeoT cells developed into lesions from which the rest of the progression series was created. These include MCF10.AT1, which models atypical hyperplasia, as well as the previously mentioned MCF10.DCIS and MCF10.Ca1D [20,21]. As xenografts, MCF10.DCIS cells form lesions that resemble premalignant comedo DCIS, which progress to IDC over time [22]. The MCF10.Ca1D cell line is one of five invasive tumorigenic cell lines derived from xenografts [23]. In a 3D environment, we show that while Rap1Gap is highly expressed in DCIS, it is downregulated in IDC. Knockdown of Rap1Gap in MCF10.DCIS cells leads to Rap1 and ERK/MAPK activation, breakdown of adherens junctions, cytoskeletal remodeling, and invasion. Introduction of dominant active (DA) Rap1A in MCF10.DCIS cells induced a similar phenotype as the Rap1Gap knockdown, and expression of a dominant negative (DN) Rap1A reversed that malignant phenotype. These results are consistent with the tumor-suppressive effects of Rap1Gap in DCIS being modulated through Rap1A activity.

Materials and Methods

Reagents

Lipofectamine 2000 and immunoblotting detection reagents were purchased from Thermo Fisher Scientific (Waltham, MA). Rabbit anti-Rap1Gap (H-93) antibody was purchased from Santa Cruz Biotechnology (Santa Cruz, CA). Rabbit anti-Rap1 (07-916) and mouse anti-GAPDH (clone C5) antibodies were purchased from EMD Millipore (Billerica, MA). Rabbit anti-total MAPK (#9102) antibody was from Cell Signaling (Danvers, MA). Mouse anti-phospho-MAPK (MAPK-YT) antibody was obtained from Sigma-Aldrich (St. Louis, MO). Mouse anti-E cadherin antibody was purchased from BD Biosciences (San Jose, CA). Mouse beta-tubulin (clone E7) antibody was obtained from the Developmental Studies Hybridoma Bank (Iowa City, IA). Reduced growth factor Cultrex reconstituted basement membrane (rBM) was purchased from Trevigen (Gaithersburg, MD).

Immunohistochemical Staining and Analysis of Patient Tissue Samples

Tissue microarrays (TMAs) BR8011 (enriched for normal and DCIS tissues), BR487 (enriched for triple-negative or TN IDCs), and BR1504 (enriched for human epidermal growth factor receptor-2 or HER2, and estrogen/progesterone receptor or ER/PR expressing IDCs) were purchased from Biomax (Rockville, MD). The slides were processed for immunohistochemistry (IHC) using optimized protocols and antibodies for Rap1Gap. Indica Labs' TMA software module (Corrales, NM) was used to segment the tissue spots on the slide and measure Rap1Gap. Paraffin sections were dewaxed in a xylene-ethanol series. Endogenous peroxides were removed by a methanol/1.2% hydrogen peroxide incubation at room temperature for 30 minutes. Heat-induced epitope retrieval was performed with a pH 6 citrate buffer in the BIOCARE Decloaking Chamber. A 1-hour blocking step with 10% goat serum in PBS was done prior to adding primary antibody (H-93 Rap1Gap antibody at 1:200 overnight). Detection was performed using Life Technologies SuperPicTure polymer Detection kit Broad Spectrum DAB (879663) or 3,3′-diaminobenzidine and counterstained with Mayer's hematoxylin. Sections were then dehydrated through a series of ethanol to xylene washes and cover slipped with Permount (Thermo Fisher Scientific). The staining for Rap1Gap was then classified as percent negative, weak, moderate, or strongly positive, taking the entire analysis region into consideration. Analysis of % positive stain of Rap1Gap was performed. Images of representative tissue spots were taken at 20× magnification.

Cell Lines and Cell Culture

MCF10 human breast epithelial progression series of cells (MCF10A, AT1, and MCF10.DCIS and MCF10.CA1D) were obtained from the Biobanking and Correlative Sciences Core at the Karmanos Center Institute, Detroit, MI. SUM 102 and SUM 225 were a generous gift from Stephen Ethier (Hollings Cancer Center, Charleston, SC). T47-D, MCF-7, MDA-MB-231, BT549, and Hs578t cell lines were obtained from ATCC (American Type Culture Collection; Manassas, VA). All cell lines were maintained as monolayer cultures with 5% CO_2. MCF10 series and SUM lines (SUM 102 and SUM 225) were maintained with DMEM/F12 supplemented with 5% horse serum and Ham's F12 growth medium supplemented with 10% fetal bovine serum (FBS), respectively. T47-D, MCF-7, and BT549 cell lines were maintained with RPMI 1640 medium supplemented with 10% FBS. Hs578T and MDA-MB-231 cell lines were maintained with DMEM growth medium supplemented with 10% FBS. Cell lines were authenticated using the STR PowerPlex 16 System (Promega) and screened for mycoplasma by microscopy (MycoFluor; Thermo Fisher Scientific) and polymerase chain reaction (PCR) (Venor GeM, Sigma-Aldrich). For 3D culture, a trypsinized single-cell suspension in 3D assay medium with 2% rBM [24] was pipetted on top of the rBM and grown for 8 days, with media change after 4 days.

Immunofluorescence

Cells were fixed and stained as described previously [25–27]. Images were collected with an LSM 780 confocal microscope (Carl Zeiss GmbH, Jena, Germany). 3D reconstructions of optical sections were generated using Volocity software v.6.3.1 as described previously [28].

RNA Extraction, Gene Expression, and Plasmid DNA Isolation

RNA extraction from cells was performed using RNeasy RNA isolation kit by Qiagen (Hilden, Germany) and Life Magnetics RNA isolation kit (Detroit, MI) from cells grown in monolayer. cDNA was synthesized using the Applied Biosystems High Capacity cDNA Reverse Transcription Kit (Thermo Fisher Scientific). All qRT-PCRs were performed using Applied Biosystems TaqMan assays (Thermo Fisher Scientific) using the Applied Biosystems StepOnePlus Real-Time PCR system. Supplemental list of TaqMan assays is in Supplementary Table 1. Plasmid DNA isolation was performed using the Bio-Rad Quantum Miniprep kit (Hercules, CA) and Life Magnetics Plasmid DNA isolation kit according to the manufacturer's instructions.

Retroviral Infection for Stable shRNA Knockdown and Transient Overexpression of Rap1Gap, DA Mutant Rap1A-V12, and DN Mutant Rap1A-N17

We targeted MCF10.DCIS cells for stable retroviral knockdown experiments using two separate shRNA sequences that target different regions on Rap1Gap. TTGGTGTGTGAAGACGTCA for kd1 (knockdown sequence 1) and TCTTCTCACTCAAG-TACG for kd2 (knockdown sequence 2) [29] were cloned into RNAi-Ready pSIREN RetroQ DsRed-Express plasmid (Takara Bio USA, Mountain View, CA) for knockdown experiments according to established protocols [25]. For transient overexpression experiments, MCF10.DCIS or MCF10.DCIS Rap1Gap shRNA cells were grown to approximately 50% confluency on 35-mm dishes and then transfected with 200 ng of GFP-Rap1Gap, GFP-Rap1A-V12, or GFP-Rap1A-N17 plasmids using Lipofectamine 2000. Parallel transfections with a control GFP plasmid [30] were also performed.

Immunoblotting

To obtain sufficient material for immunoblotting, 3D overlay cultures were set up on 60-mm culture dishes and grown for 8 days. Structures were harvested from rBM by repeated washes with ice-cold PBS supplemented with 5 mM EDTA. Lysates were prepared, separated by SDS-PAGE, transferred to nitrocellulose membranes, and immunoblotted with the appropriate antibodies following the protocols previously described [25,26]. We performed Bradford's

protein assay in order to determine the appropriate amount of protein for loading.

Invasion Assays

Thirty thousand MCF10.DCIS or MCF10.DCIS Rap1Gap shRNA cells were seeded in serum-free media on BD cell culture inserts (8-μm pore size; Franklin Lakes, NJ) that we precoated with 2 mg/ml Cultrex. Cells were allowed to invade for 24 hours toward media supplemented with 5% horse serum. After removing the noninvading cells with a cotton swab, the cells that had invaded through the filter were stained, and the filters were mounted on slides using a Dif-Quik kit (Thermo Fisher Scientific). The cells were then visualized using a Zeiss Axiovert-200 microscope and counted using ImageJ software (NIH). Data were collected from four independent experiments performed in triplicate.

Rap1 Activity Assay

Rap1 activity assays were done according to the manufacturer's instructions (EMD Millipore). Briefly, whole cell lysates were prepared in ice-cold lysis buffer [50 mmol/l Tris-HCl (pH 7.4), 0.5 mol/l NaCl, 1% NP40 (v/v), 2.5 mmol/l $MgCl_2$, 10 μg/ml aprotinin, 10 μg/ml leupeptin, and 10% glycerol]. Ral GDS-RBD agarose beads were used to pull down active Rap1 for 45 minutes at 4°C. Samples of the pulldowns and of the input lysates were separated by SDS-PAGE, transferred, and immunoblotted for Rap1.

Results

High Expression of Rap1Gap in MCF10.DCIS and Luminal Hormone-Responsive Cells

Previous studies from our laboratory determined gene expression changes common to three models of DCIS cells grown in 3D cultures in comparison to nontransformed MCF10A cells, also grown in 3D. Next-generation sequencing results showed that Rap1Gap was upregulated in all three cell models of DCIS compared to MCF10A cells [31]. To confirm whether protein expression correlated with the mRNA, we performed immunoblotting for Rap1Gap in the MCF10 human breast progression series and in SUM 102 and SUM 225 lines (Figure 1). In the progression series, MCF10A cells expressed very low levels of Rap1Gap; MCF10NeoT, a model of transformed breast epithelium, and MCF10.AT1, a model of atypical hyperplasia, expressed some Rap1Gap; MCF10.DCIS, a model of DCIS, expressed high levels of Rap1Gap as expected from the previous transcriptomic analysis; and MCF10.Ca1D, a model of IDC, expressed very low levels of Rap1Gap. In the two other DCIS lines (SUM 225 and SUM 102), Rap1Gap levels were strikingly different, although prior transcriptomic analysis identified the upregulation of Rap1Gap mRNA in both [31]. SUM 225 cells, a HER2 overexpressing line that exhibits luminal markers and was derived from a chest wall recurrence in a patient previously diagnosed with DCIS [32], abundantly expressed Rap1Gap to a level similar to that found in MCF-7 cells, which have previously been characterized to have high expression [33]. In contrast, SUM 102 cells, which are of basal type and were derived from a DCIS with microinvasion [34,35], expressed very low levels of Rap1Gap.

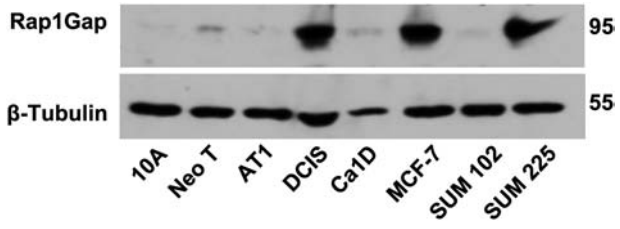

Figure 1. Rap1Gap protein is highly expressed at DCIS stage of the MCF10 progression series and SUM 225 cell lines. Lysates were prepared from cells grown on rBM for 8 days. Expected molecular weight of Rap1Gap is 95 kDa. MCF-7 served as a positive control for expression of Rap1Gap protein. β-Tubulin was used as a loading control. Data are representative of three separate experiments.

High Levels of Rap1Gap in Human DCIS compared to Normal and IDC Breast Tissue

To confirm the spectrum of Rap1Gap expression found in human patient samples, we performed IHC for Rap1Gap in tissue microarrays (Figure 2). The results confirmed that Rap1Gap is significantly overexpressed in patient samples of DCIS relative to both the normal-adjacent and IDC samples. The TMAs included 36 samples of normal/tumor adjacent breast tissue, 50 samples of DCIS/intraductal carcinoma, and 179 samples of IDC. One-way analysis of variance (ANOVA) and Bonferroni's test for multiple comparisons show statistically significant differences in the Rap1Gap expression between DCIS and normal or IDC tissues (normal vs. DCIS, $P = 0.0307$; DCIS vs. IDC, $P = 0.0004$). When the IDC samples were separated into ER+/PR+, HER2+, and TN subtypes (Figure S1), we found that expression of Rap1Gap was significantly reduced in the ER+/PR+ IDC samples relative to DCIS and that there was a trend (not reaching significance) for a reduction in Rap1Gap expression in TN IDC relative to DCIS (Figure S1*F*). The TMAs included 75 samples of ER/PR+, 31 samples of HER2+, and 86 samples of TN IDCs. Samples with 1% positive staining for ER/PR were considered to be ER/PR+. To be considered HER2+, we included samples that were reported to have 3+ expression. Biomarker expression (ER/PR, HER2, etc.) profiles for each tissue spot in the TMAs were provided by Biomax. One-way ANOVA and Bonferroni's test of multiple comparisons show statistically significant differences in Rap1Gap expression between DCIS and subtypes of IDC (DCIS vs. ER+/ER+ IDC; $P < 0.0001$).

Rap1Gap protein levels were also assessed in breast IDC cell lines. We found a clear difference with regard to breast cancer subtype (Figure S1*G*). Rap1Gap is expressed at higher levels in the luminal A hormone-responsive cell lines (MCF-7 [36,37] and T47-D [37]) and at lower levels in the basal B breast cancer cell lines (MDA-MB-231, Hs578t and BT549), which have mesenchymal characteristics [38,39].

Alteration of Cell Morphology from Epithelial to Mesenchymal Phenotype: A Consequence of Rap1Gap Silencing in MCF10.DCIS

As expression of Rap1Gap in breast IDC cell lines with mesenchymal characteristics was low, we hypothesized that Rap1Gap might act as a limiting factor on the progression of DCIS to IDC and that knocking down Rap1Gap in MCF10.DCIS cells would confer mesenchymal characteristics, including changes to a spindle shape and an invasive phenotype. Figure 3 shows MCF10.DCIS cells

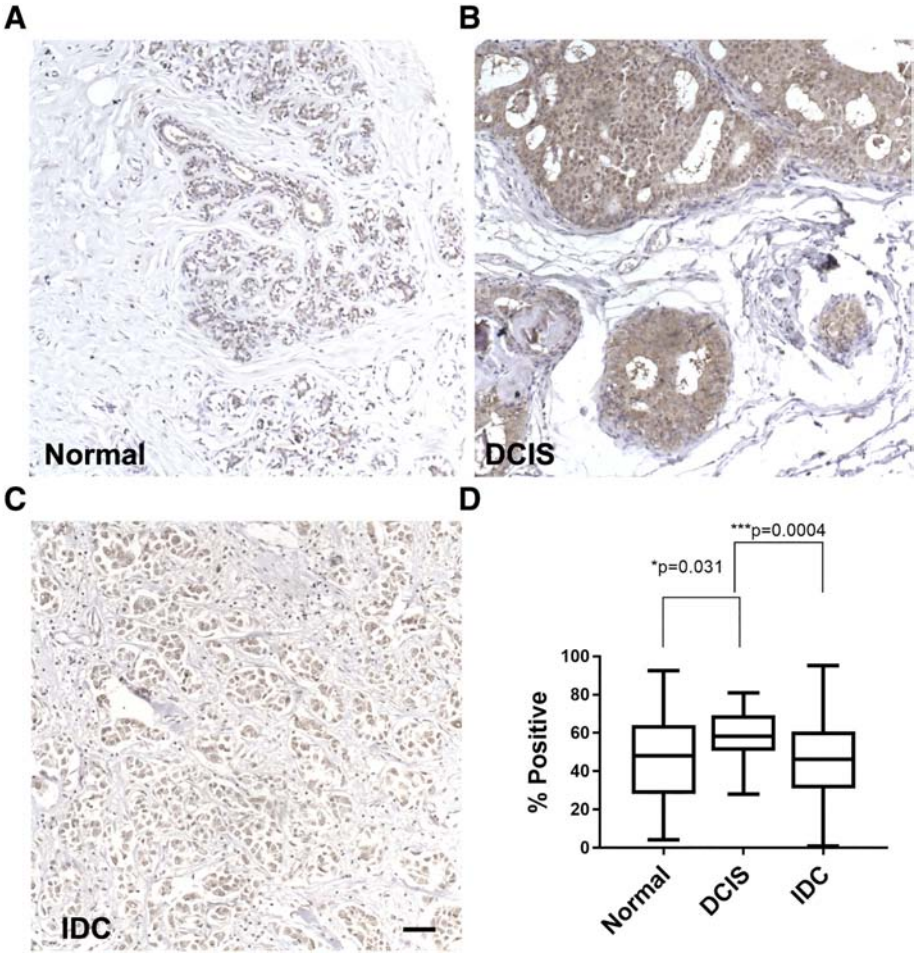

Figure 2. Rap1Gap is reduced in normal and human IDC patient samples relative to DCIS samples. The TMAs included 36 samples of normal/tumor adjacent breast tissue, 50 samples of DCIS/intraductal carcinoma, and 179 samples of IDC. The slides were processed for IHC. (A-C) Representative panels of Rap1Gap expression in normal (A), DCIS (B), and IDC(C) tissue. Images were taken at 20×. Size bar is 50 μm. (D) Data are represented as box and whisker plots, where the box represents the interquartile range and whiskers represent minimum and maximum values. One-way ANOVA and Bonferroni's test for multiple comparisons show statistically significant differences in the Rap1Gap expression between DCIS and normal or IDC tissues (normal vs. DCIS, $P = 0.0307$; DCIS vs. IDC, $P = 0.0004$).

infected with pSIREN dsRed retroviral control and two separate shRNA sequences that target Rap1Gap (termed kd1 and kd2). In 2D culture, MCF10.DCIS cells grow in clusters with an epithelial phenotype and cell-cell contacts. Knockdown of Rap1Gap in MCF10.DCIS altered cellular shape toward a more scattered fibroblastic phenotype, with less frequent cell-cell contacts (Figure 3*A*). Immunoblotting confirmed that both shRNA sequences were highly effective at reducing Rap1Gap expression (Figure 3*B*).

One characteristic of invasive breast cancer and mesenchymal phenotype is reduced E-cadherin and breakdown of adherens junctions [40–42]. For example, E-cadherin is lost in invasive mesenchymal breast cancer cell lines [42,43], which also expressed low levels of Rap1Gap (Figure S1). We hypothesized that reduction in E-cadherin and fewer adherens junctions would be a consequence of Rap1Gap knockdown. E-cadherin localization consistent with adherens junctions was present in the retroviral control MCF10.DCIS cells in 3D cultures but missing following knockdown of Rap1Gap (Figure 4*A*). In addition to changed localization, expression of E-cadherin was also reduced following Rap1Gap knockdown (Figure 4*B*). Localization of E-cadherin to cell:cell junctions in control MCF10.DCIS cells was also shown clearly in 2D cultures (Figure S2) and is consistent with our previous studies [27]. Reduction in E-cadherin following Rap1Gap knockdown was also observed in monolayer cultures. This localization of E-cadherin was reduced following knockdown of Rap1Gap.

Loss of Rap1Gap: Formation of Multicellular Outgrowths, Cytoskeletal Remodeling, and Invasion

When grown in rBM, MCF10.DCIS cells form compact dense and dysplastic structures ([25] and Figure 4*A*). We hypothesized that MCF10.DCIS Rap1Gap shRNA cells would gain an invasive phenotype that would be revealed in 3D cultures by production of multicellular outgrowths. After 8 days of growth in rBM, the 3D structures formed by MCF10.DCIS Rap1Gap shRNA cells were less densely packed (Figure 4*A*), were larger (Figure 4*C*), and exhibited a significant increase in the number of multicellular invasive outgrowths (Figure 4*C*, *D*). One-way ANOVA and Kruskal-Wallis test for multiple comparisons were performed to show the statistically significant differences between the number of outgrowths in the control vs. both of the knockdown lines; $P < 0.0001$.

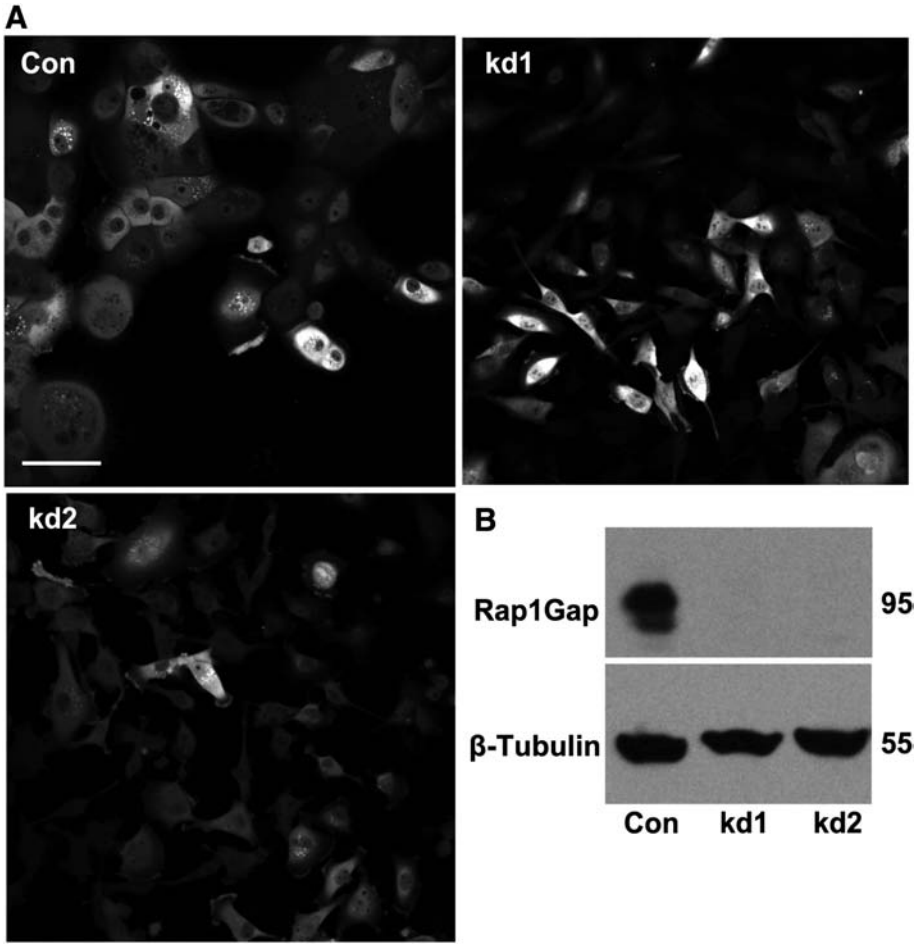

Figure 3. Rap1Gap knockdown in MCF10.DCIS cells transforms cellular morphology from epithelial to mesenchymal phenotype. (A) MCF10.DCIS cells grown in monolayer cultures were infected with pSIREN dsRed control (Con) or Rap1Gap shRNA (kd1 and kd2). Images (20× magnification) are shown in gray scale to better delineate morphology. Size bar, 50 μm. (B) The immunoblot shows robust knockdown of Rap1Gap using two separate shRNA sequences. β-Tubulin was used as a loading control.

These morphological changes are also shown in the 3D reconstructions in Figure 5*A* and in the supplementary movie files. There was an overall change in the organization of the actin cytoskeleton, with the outgrowths containing actin stress fibers, as observed in the images of the collapsed *z*-stacks (Figure S3). These images also show that the cortical actin rings that are found in MCF10.DCIS cells were lost following knockdown of Rap1Gap.

Cytoskeletal remodeling is a significant part of the invasion process and is carefully orchestrated [44,45]. In order to test whether loss of Rap1Gap would enhance the invasive capability of MCF10.DCIS cells, the ability of the cells to move through rBM was assayed. We found a significant increase in the number of invading cells when Rap1Gap is silenced, compared to the control (Figure 5*B*, *C*). One-way ANOVA and Dunn's multiple comparisons test were performed for statistically significant differences between the number of invaded cells in the control vs. the two knockdown lines; $P = 0.0002$. Live cell proteolysis assays were also performed to test whether this invasive phenotype was associated with an increased ability to degrade the matrix. Degradation of collagen IV (indicated by green fluorescence) was detected in the MCF10.DCIS Rap1Gap shRNA structures but not in control MCF10.DCIS structures (Figure S4).

Rap1Gap Silencing in MCF10.DCIS: Increase in ERK/MAPK Activation

ERK/MAPK activation has been observed in a wide variety of cancers and is closely associated with cancer development, migration, invasion, and metastasis [46]. In IDC, ERK/MAPK mediates migration and invasion [47]. Our results (Figure 5*C*) show that silencing of Rap1Gap in MCF10.DCIS led to enhanced invasion. Therefore, we hypothesized that Rap1Gap silencing may result in ERK/MAPK activation in MCF10.DCIS cells. The immunoblotting results in Figure 6*A* show increased phosphorylation of ERK1/2 in MCF10.DCIS cells with silenced Rap1Gap expression. A 6-fold and 12-fold increase in ERK1/2 phosphorylation was observed in the kd1 and kd2 lines, respectively, compared to the control. We also observed robust ERK1/2 activation in 3D cultures of MCF10.Ca1D cells compared to the control (a 14-fold increase). Significant differences in activated ERK1/2 between the control and the knockdown lines or MCF10.Ca1D cells were assessed using one-way ANOVA and Bonferroni's multiple comparisons test; $P = 0.0006$.

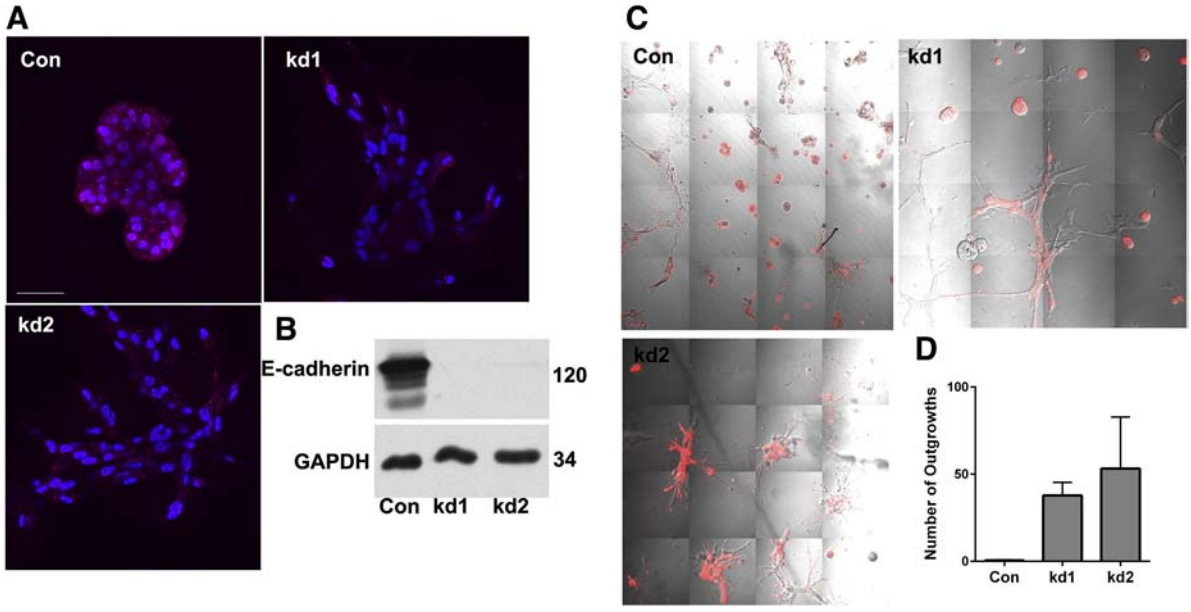

Figure 4. Knockdown of Rap1Gap expression in MCF10.DCIS cells reduces E-cadherin levels and leads to development of multicellular outgrowths in 3D cultures. (A) DCIS retroviral control and DCIS Rap1Gap shRNA cells were grown in rBM for 8 days and fixed. Images are four confocal contiguous fields taken at 63× at equatorial position. Red is immunofluorescent detection of E-cadherin, and DAPI (blue) is of DNA. Size bars are 50 μm. (B) Immunoblot shows E-cadherin expression isolated from cells grown in monolayer culture for 5 days. GAPDH is loading control. (C) After growing for 8 days, differential interference contrast (DIC) images, consisting of 16 contiguous fields, were taken at 20× magnification. Images are representative of three separate experiments. The red fluorescence is the dsRed reporter protein present in the control and Rap1Gap knockdown plasmid. (D) Outgrowths were counted by two blinded individuals. One-way ANOVA and Kruskal-Wallis test for multiple comparisons were performed to show the statistically significant differences between the number of outgrowths in the control vs. both of the knockdown lines. $P < 0.0001$. Error bars represent standard error of the mean (SEM).

Reexpression of Rap1Gap in MCF10.DCIS Rap1Gap shRNA Cells: Decrease in Rap Activation and Block of Malignant Phenotype

To further test the role of Rap1Gap in the transition of MCF10.DCIS to an invasive phenotype, we performed rescue experiments. We hypothesized that reexpression of Rap1Gap would decrease Rap activity and block the formation of invasive multicellular outgrowths in 3D structures formed by the Rap1Gap knockdown lines. A GFP-Rap1Gap construct was transfected into DCIS Rap1Gap kd2 shRNA cells. To test expression of GFP-Rap1Gap, cells were grown in 2D

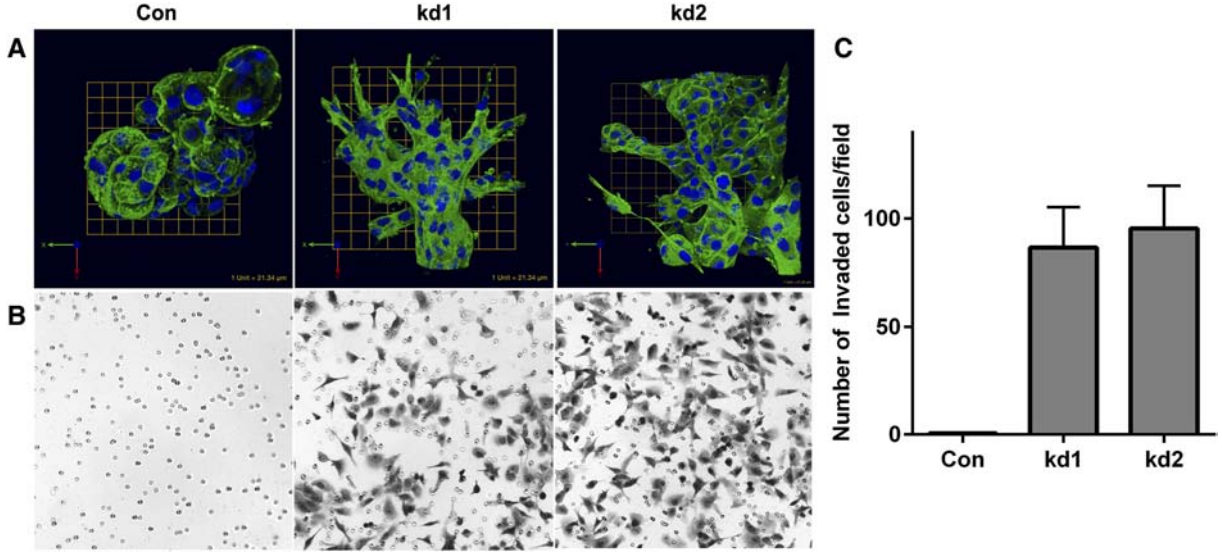

Figure 5. Knockdown of Rap1Gap expression in MCF10.DCIS cells leads to cytoskeletal remodeling and invasion. (A) Images (40× magnification) are snapshots of 3D reconstructions of *z*-stacks of overlaid green and blue channels. Green is fluorescent detection (FITC Phalloidin) of F-actin, and DAPI (blue) is of DNA. Movie files of the 3D reconstructions are included as supplementary data. (B) Images (20× magnification) are of cells that invaded through the filter. (C) Graph shows mean number of invaded cells ±SEM. Data set is the mean of four independent experiments done in triplicate. One-way ANOVA and Dunn's multiple comparisons test were performed for statistically significant differences between the number of invaded cells in the control vs. the two knockdown lines; $P = 0.0002$.

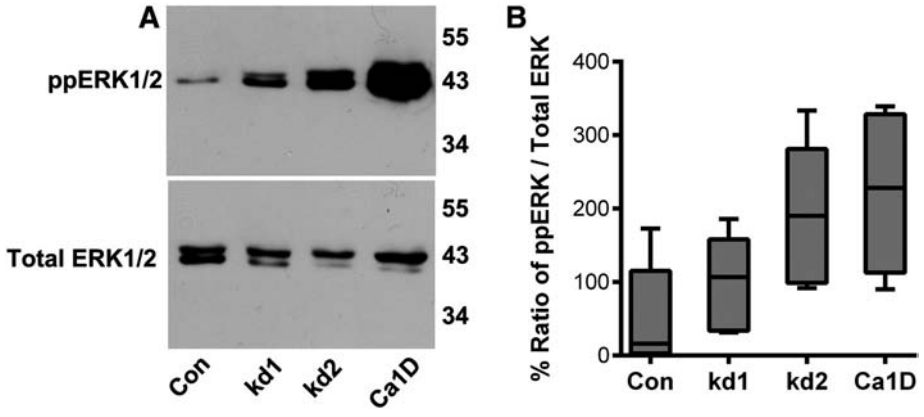

Figure 6. Rap1Gap knockdown in MCF10.DCIS causes an increase in ERK/MAPK activation. (A) Immunoblot of ERK1/2 in lysates prepared from cells grown in 3D shows ERK1/2 activation in the DCIS knockdown lines and MCF10.Ca1D cells vs. the control. (B) ERK1/2 activation was quantified using densitometry and plotted using GraphPad Prism. Box whisker plot shows percent ratio of phosphorylated ERK1/2 vs. total ERK1/2 from immunoblots from four separate experiments. Significant differences in activated ERK1/2 between the control and the knockdown lines or MCF10.Ca1D cells was assessed using one-way ANOVA and Bonferroni's multiple-comparisons test; $P = 0.0006$.

conditions for 3-5 days before imaging (Figure S5*A*), and lysates were prepared for immunoblotting (Figure 7*B*); both confirmed successful reexpression. Transfected cells from parallel dishes were trypsinized and seeded directly on rBM to be cultured with overlay for 8 days before fixing and staining for F-actin (Figure 7*A*). Reexpression of Rap1Gap blocked development of invasive outgrowths and restored

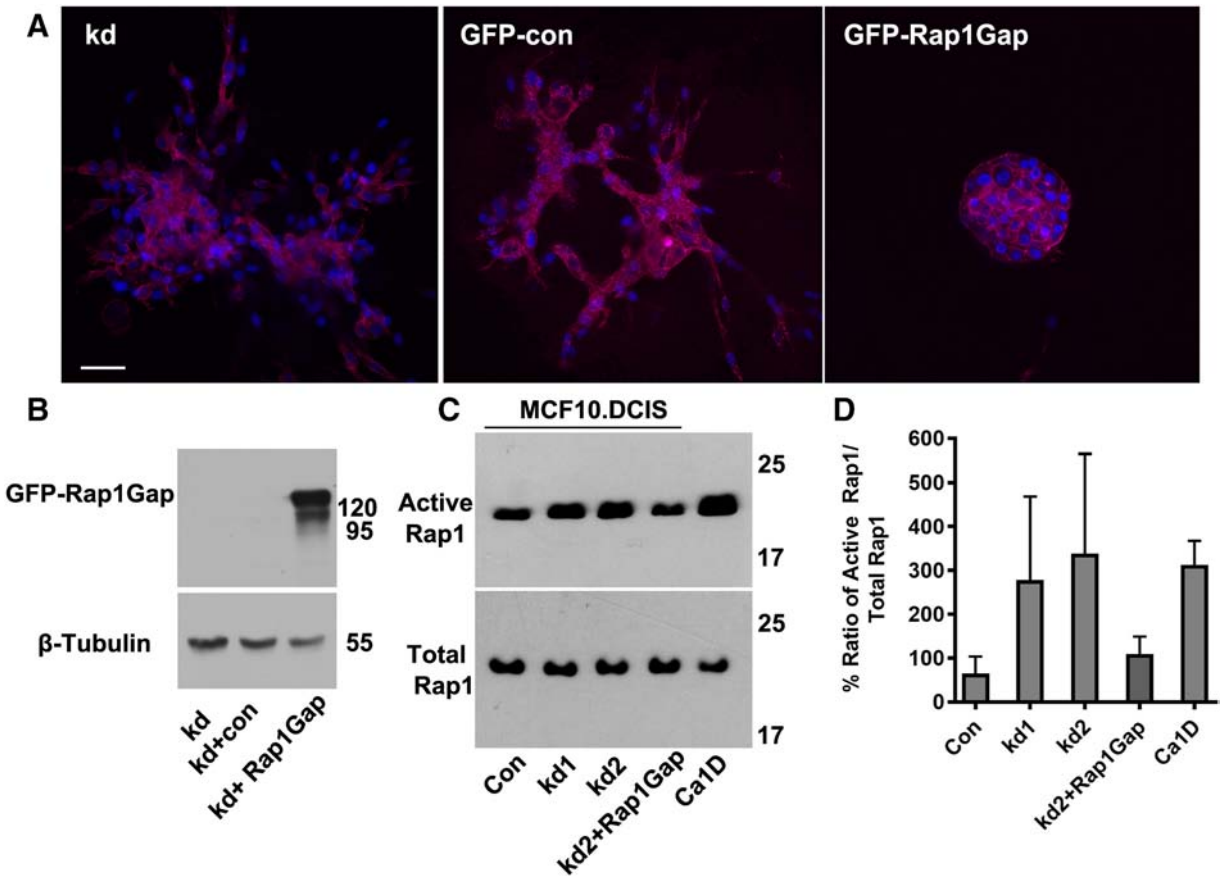

Figure 7. Rap1Gap reexpression in MCF10.DCIS Rap1Gap shRNA cells decreases Rap1 activity and blocks mesenchymal phenotype. (A) Shown in magenta, fluorescent probe detection of filamentous actin in the kd2 line, GFP control (GFP-con), and kd2 line with GFP-Rap1Gap expression. DAPI (blue) is fluorescent detection of DNA. Images are representative of three separate experiments. A 63× image of F-actin cortical rings (magenta) in the kd2 lines expressing GFP-Rap1Gap is shown in Figure S5*B*. (B) Immunoblot shows robust reexpression of GFPRap1Gap fusion protein in kd2 following transfection. (C) Increased Rap1 activity in the Rap1Gap shRNA cells and in MCF10.Ca1D cells. Reexpression of Rap1Gap in kd2 cells leads to reduction of Rap1 activity similar to the control. (D) Bar graph of percent ratio of Rap1 GTP vs. total Rap1. Data are mean ± SD taken from two separate experiments.

the compact and dense phenotype that is characteristic of the 3D structures formed by MCF10.DCIS cells. Actin cortical rings were also restored by reexpression of Rap1Gap (Figure S5*B*).

Given that Rap1Gap is a negative regulator of Rap, we reasoned that knockdown of Rap1Gap would result in an increase in Rap activity and that reexpression of Rap1Gap would reverse that activation. As seen in Figure 7*C*, *D*, while modest Rap1 activity was observed in the control MCF10.DCIS cells, increased Rap1 activity was found in both of the MCF10.DCIS Rap1Gap shRNA lines (four- and five-fold, respectively, compared to the control cells) and in MCF10.Ca1D cells (a five-fold increase). In addition, reexpression of Rap1Gap caused a reduction in Rap1 activity (three-fold) in the kd2 line.

Effects of DA-Rap1A and DN-Rap1A on Malignant Phenotype

Rap1Gap is a negative regulator of Rap1A and Rap1B [16]. Given that knockdown of Rap1Gap led to Rap1 activation and subsequent acquisition of invasive phenotype, we investigated whether direct modulation of Rap1A activity would have similar effects. Transient transfection of GFP-tagged DN-Rap1A mutant (Rap1A-N17) in the kd2 line led to the appearance of cell-cell contacts in monolayer culture and clustering of cells (see Supplemental Figure S6). When grown in 3D (Figure 8), expression of DN-Rap1A mutant (Rap1A-N17) in the kd2 line led to a reversion of invasive phenotype and the reappearance of organized cortical rings and compact structure (Figure S7), similar to MCF10.DCIS. The images in Figure S7 also show disorganized cortical rings in the 3D structures formed by the MCF10.DCIS cells after transfection with the DA Rap1A. The 3D structures, formed by the MCF10.DCIS cells when transfected with DA Rap1A mutant (Figure 8), lost their characteristic compact shape, displayed disorganization of the actin cytoskeleton, and grew invasive outgrowths, a phenotype that is reminiscent of the kd2 line (Figure 5).

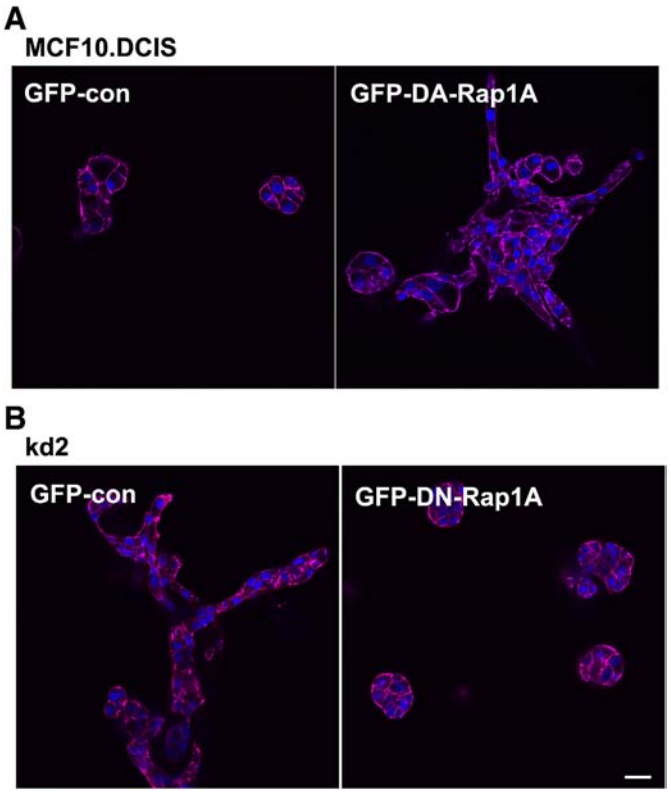

Figure 8. Expression of dominant active (DA) Rap1 (Rap1-V12) in MCF10.DCIS cells and dominant negative (DN) Rap1A (Rap1A-N17) in MCF10.DCIS Rap1Gap shRNA (kd2) cells promotes and blocks mesenchymal phenotype, respectively. (A) Shown in magenta, fluorescent probe detection of filamentous actin in MCF10.DCIS cells transfected with GFP control (GFP-con) and GFP-DA-Rap1A. (B) Fluorescent probe detection of filamentous actin in the kd2 line transfected with GFP-control and GFP-DN-Rap1A. DAPI (blue) is fluorescent detection of DNA. Images were taken at 20× magnification and are representative of three separate experiments. Size bar is 20 μm. Please see Figure S7 for 40× images of F-actin cortical rings (magenta) in the MCF10.DCIS cells transfected with GFP control plasmid and kd2 lines expressing GFP-DN-Rap1A, respectively.

Discussion

We aimed to delineate the role of Rap1Gap in the progression to IDC by using the MCF10 progression series as a model. Our previous transcriptomic data [7] revealed that Rap1Gap was upregulated in MCF10.DCIS and two other DCIS lines, SUM 225 (derived from a chest wall recurrence [32]) and SUM 102 (a primary DCIS with microinvasion [7,34,35]), compared to the nontransformed MCF10A cells. Our immunoblotting analysis confirmed that Rap1Gap expression is high in MCF10.DCIS and SUM 225 cells but unexpectedly found low expression of Rap1Gap in SUM 102 cells. This might be due to the dynamic regulation of Rap1Gap protein stability, as occurs in thyroid cancer models [48]. Our IHC analysis of breast tissue samples revealed that DCIS lesions had a higher percentage of Rap1Gap expressing cells compared to normal tissue. These results are consistent with our *in vitro* data on the MCF10 progression series (Figure 1) and with IHC of tissues in the Protein Atlas website (http://www.proteinatlas.org/ENSG00000076864-RAP1GAP/tissue). The latter reports positive staining for Rap1Gap in the majority (9 of 11) of the small set of DCIS samples, with nondetectable staining in normal tissue.

Analysis of Rap1Gap staining in the IDC samples revealed an overall reduction in Rap1Gap expression compared to that in DCIS samples. Analysis of Rap1Gap staining profiles in IDCs divided by subtype revealed that Rap1Gap is reduced in ER+/PR+ IDCs and a downward trend for its expression in TN IDCs compared to DCIS. Even though our staining analyses show reduced Rap1Gap in the ER+/PR+ IDCs compared to other subtypes, we found high Rap1Gap expression levels in two cell lines, MCF-7 and T47-D, that model luminal A [37], hormone-responsive disease. The overall pattern of the tissue expression included a large range of intersample variability, and thus, it may be that these two cell lines represent cases at the upper range of Rap1Gap expression.

The variability in Rap1Gap expression in our panel of breast cancer cell lines and within the IDC subtypes used in our TMA analysis could be related to the molecular heterogeneity and clinicopathological features present in DCIS and IDC [49,50]. Reports have proposed that molecular features (gene signatures) associated with disease progression are characteristic of five intrinsic subtypes [51]. It is possible that Rap1Gap expression profiles in breast cancer might be subtype specific. There was a trend of decreased Rap1Gap expression in the TN IDC cases relative to DCIS, but that did not reach significance perhaps because of the few TN IDC samples available for analysis (N = 86). It will be useful to further explore that potential pattern because there was a consistent pattern in the TN IDC cell

lines, with the three tested showing low Rap1Gap expression. A further complication is that the TN category includes subsets of disease that are marked by significant molecular heterogeneity [52–56]. The TN cell lines studied here (BT549, Hs578T, and MDA-MB-231) [37,38] are primary breast papillary IDC, carcinosarcoma, and adenocarcinomas, respectively (see Table 1 of [57]). They express low levels of claudins [37] and exhibit gene expression profiles that are enriched for mesenchymal markers [58,59]. Thus, low levels of Rap1Gap may be particularly associated with the claudin low subset of TNBCs and thus be linked with acquisition of mesenchymal characteristics.

Our results are also consistent with gene expression data obtained from the Oncomine database. The Curtis Breast dataset shows a 2.4-fold increase in Rap1Gap mRNA expression in DCIS samples compared to normal breast tissue samples (Figure S8). Interestingly, the same dataset shows a 1.69-fold change decrease in Rap1Gap mRNA expression in TN IDCs vs. IDCs with other biomarkers (Figure S9). The TCGA Breast dataset also reveals that Rap1Gap mRNA expression is downregulated 1.43-fold in TN IDC samples compared to IDCs expressing other biomarkers (Figure S10).

Our results (Figures 3-5, 7) indicate that, upon silencing of Rap1Gap, MCF10.DCIS cells acquired phenotypic and behavioral characteristics that are reminiscent of the basal B cell lines BT549, MDA-MB-231, and Hs578T [38,39]. In particular, when grown in rBM, basal-like cell lines display a stellate phenotype, characterized by reduced or absent E-cadherin, and/or presence of multicellular outgrowths [57]. They also demonstrate robust invasive capability in *in vitro* assays and exhibit activated ERK/MAPK signaling [57]. Here we demonstrated that silencing of Rap1Gap in MCF10.DCIS cells results in activation of ERK MAP kinase, reduced levels of E-cadherin, formation of invasive outgrowths (cytoskeletal remodeling), and a robust invasive capability. These data are strongly supported by other studies which have previously reported that depletion of Rap1A in aggressive breast cancer cell line MDA-MB-231 reduces invasion in 3D Matrigel cultures [60]. These results also are in line with other reports where, in colon cancer models, increased Rap1 activation leads to breakdown of adherens junctions, cytoskeletal remodeling, and enhanced invasion [19,29,61]. Our results also complement observations where overexpression of Rap1Gap decreases invasive capability of renal cell carcinoma cell lines [18].

Epithelial to mesenchymal transition (EMT) is a complex, transient, and reversible process, characterized by the loss of epithelial characteristics (such as cell-cell attachments, adhesion, and apical-basal polarity) and the gain of mesenchymal characteristics (such as increased motility, invasive properties, and a spindle-like morphology) [62]. Loss of functional E-cadherin contributes to an EMT-like phenotype, in which epithelial cells exhibit loss of cell-cell adhesion, increased motility, and invasiveness [63]. While studies have linked Rap1 to formation of E-cadherin–based cell-cell contacts [64], reciprocal interactions include Rap1 linkage to E-cadherin endocytosis [65] and disengagement [66]. Our data are in agreement with a recent study correlating low levels of Rap1Gap with loss of E-cadherin expression and EMT in gastric cancer [67]. Other studies also show that downregulation of Rap1Gap has been linked to invasion and/or EMT in multiple cancers [15–17,29,67,68] and is correlated with induction of mesenchymal morphology and migratory behavior [69]. Epithelial cells possess apicobasal polarity, which helps anchor them to the basement membrane [70]. EMT-like changes include the transition from apicobasal polarity to front-rear polarity and loss of cortical actin rings with gain of actin stress fibers [71]. We have shown that while MCF10.DCIS cells have cortical rings, Rap1Gap shRNA cells do not and instead develop stress fibers in the cells in the invasive outgrowths. Thus, our studies link Rap1 activation and alterations in adherens junctions *via* reduction in E-cadherin. Our studies also connect changes in cytoskeletal remodeling to mesenchymal morphology and invasion.

Silencing of Rap1Gap in MCF10.DCIS cells led to increased ERK/MAPK phosphorylation in 3D models of DCIS. This observation is in line with 2D studies in melanoma cells that show that Rap1Gap overexpression leads to reduced ERK/MAPK phosphorylation [15]. In the context of IDC, our findings are in agreement with ERK/MAPK mediating cell migration and invasion [47]. Previous studies from our laboratory have confirmed the presence of activated H-Ras in MCF10.DCIS [27]. This is expected because MCF10.DCIS is isogenic to the MCF10.NeoT cell line, which harbors the constitutively active T24-H-Ras [21], and thus, DCIS Rap1Gap shRNA cells also express constitutively active H-Ras. Because ERK/MAPK is further activated in the DCIS Rap1Gap shRNA cells, we conclude that Rap1 and Rap1Gap might participate downstream of Ras to control the activation of ERK/MAPK. For example, Rap1 may regulate ERK/MAPK by antagonizing signals relayed by H-Ras. Other studies have supported a role for Rap1 in inhibition of transformation by Ras due to its participation in signaling networks that control cell polarity [72] and strengthening of cell attachment to both extracellular matrix and neighboring cells [73]. Other studies have reported that overexpression of Rap1A in ovarian cancer cells led to ERK1/2 activation and enhanced expression of EMT markers [74]. Conversely, the MEK inhibitor U0126 reversed the effects of Rap1A *via* ERK1/2 inhibition. These data build upon previous work in endothelial cells, where similar effects were observed when introduction of DN-Rap1A reduced ERK1/2 phosphorylation and led to concomitant reduction tube formation, proliferation, and migration [14].

Rap1A mRNA is robustly expressed in DCIS and IDC samples compared to normal mammary ductal cells, and Rap1A protein levels are increased in invasive breast cancer cell lines vs. MCF7 and MCF10A cells [60]. We show that introducing DN-Rap1A does phenocopy the effects of Rap1Gap expression on DCIS cells. We further show that introducing DA-Rap1A in premalignant DCIS cells leads to the acquisition of an invasive phenotype (Figure 8), which mimics the phenotype observed in the kd2 line (Figures 4 and 5). Our qRT-PCR analyses reveal measurable expression of mRNAs for Rap1A, Rap1B, and Rap2 in MCF10.DCIS cells. Thus, although our data show that manipulation of Rap1A activity can phenocopy changes in Rap1Gap expression, it is possible that Rap1B and/or Rap2 might play a role in this system and could be the subject of further studies. Rap1B and Rap2 expression is associated with poor prognosis, aggressive phenotype, and metastasis in various cancers [75,76]. Thus, overall, we conclude that upregulation of Rap1Gap in MCF10.DCIS, through modulation of Rap activity, might serve as a tumor-suppressive attempt to prevent progression to IDC by reducing Ras-driven transformation. This is consistent with the role of Rap1 as an antagonist of activated Ras in thyroid cancer [77].

Various studies suggest that Rap1Gap may function as tumor suppressor since it is frequently lost in several tumor types [48]. Tumor suppressors serve as transducers of antiproliferative signals, inhibit cell cycle progression, and induce apoptosis [78]. Overexpression of Rap1Gap in various cell types induces apoptosis [79],

inhibits cell proliferation [14,16], blocks passage through the cell cycle [80], and reduces tumor progression [68,69]. Studies in various models, such as melanoma and thyroid and pancreatic cancers, show that Rap1Gap expression is lost at a higher frequency in more aggressive tumor types *via* promoter hypermethylation and/or loss of heterozygosity (LOH) [15,17,68,81]. LOH for Rap1Gap leads to promotion of growth, survival, and invasion in pancreatic cancer models *in vitro* and *in vivo* [17]. These findings are complemented by studies in prostate cancer that show evidence of cancer cell migration, invasion, and enhanced rate of tumor incidence in mouse xenograft models following Rap1 activation [82]. Additional *in vivo* experiments performed to evaluate the tumor-suppressive effect of Rap1Gap show reduction in tumor size, inhibition of tumor formation, and fewer metastases following reexpression [16,17]. Moreover, clinical studies in endometrial cancer show that low levels of Rap1Gap are correlated with poorly differentiated tissue [67]. Thus, Rap1Gap possesses the majority of the well-studied characteristics found in tumor suppressors, which suggests that Rap1Gap may function in this manner in the progression to IDC.

Alternative signaling mechanisms for the role of Rap1Gap in cancer progression have been proposed. Recent investigations on the effects of Rap1Gap on human umbilical cord vein endothelial cells reveal inhibition of proliferation *via* ERK/MAPK and protein kinase B (AKT) pathways [14]. Additionally, studies show that overexpression of Rap1Gap in pancreatic cancer cells lines [17] resulted in inhibition of focal adhesion kinase activation and cell spreading without changes in ERK/MAPK phosphorylation. Other studies have also shown that depletion of Rap1Gap in colon cancer cells induces increase in Src and focal adhesion kinase activation [29]. Rap1 also affects the endocytic recycling pathway involved in the formation and maintenance of E-cadherin–mediated cell-cell junctions in human embryonic stem cells [83]. In addition to the regulation of E-cadherin, inside-out signaling *via* the integrins, which link the ECM to the actin skeleton at focal adhesion sites, is also regulated by Rap1 *via* Src activity [84]. Rap1 also spatially and temporally regulates actin dynamics *via* Rho in endothelial barrier function [85]. This might be germane to the mechanism of stress fiber formation in mammary epithelial cells and would be in line with previous studies from our laboratory that suggested that increased Rho A activity might be a contributing factor to the fibroblastic phenotype in Ras-transformed MCF10A cells [27]. Since a more mesenchymal phenotype was observed in the MCF10.DCIS cells with silenced Rap1Gap, it is possible that increased Rap1 activity might lead to increased RhoA activity, resulting in stress fiber formation and facilitation of the process of invasion.

Rap1Gap is member of a family of proteins that regulate Rap1. Rap1Gap2 is expressed in normal luminal cells and myoepithelial cells of the human breast duct (https://www.proteinatlas.org/ENSG00000132359-RAP1GAP2/tissue/breast). We did not find other reports describing Rap1Gap2 expression in breast cancer, but our qRT-PCR analyses identified mRNA for Rap1Gap2 in the MCF10.DCIS cells. Signal-induced proliferation-associated 1 (SIPA1), another member of the Rap1Gap family of proteins, is reported to be involved in breast cancer progression. SIPA1 is expressed in human ductal and myoepithelial cells (https://www.proteinatlas.org/ENSG00000213445-SIPA1/tissue/breast), although our qRT-PCR analysis indicated very low mRNA expression levels in MCF10.DCIS cells. Thus far, the majority of studies that have linked *SIPA1* to breast cancer are analyses of single nucleotide polymorphisms and their correlation with breast cancer risk, incidence, metastasis, and poor prognosis and survival [86–89]. One group has recently reported that nuclear SIPA1 activates the promoter of β1 integrin and promotes invasion of MDA-MB-231 breast cancer cells [90].

This is the first mechanistic study of Rap1Gap in breast cancer progression. Decreases in Rap1Gap expression led to changes in adherens junctions *via* reduction in E-cadherin levels, to cytoskeletal remodeling, and to increases in ERK activation that are correlated with an invasive phenotype in DCIS (see model in Graphical Abstract). We have developed a model in which high expression of Rap1Gap may be limiting the premalignant progression of breast cancer at the DCIS stage, whereas subsequent reduction in Rap1Gap may act as a switch to an invasive phenotype.

Supplementary data to this article can be found online at https://doi.org/10.1016/j.neo.2018.07.002.

Acknowledgements

We thank Judy Meinkoth (University of Pennsylvania, PA) for her generous gift of Rap1Gap antibody and critical reading of the manuscript. We also thank Patrick Casey (Duke-NUS Medical School, Singapore) for his generous gift of the GFP-Rap1Gap plasmid. We also thank Mark R. Philips (New York University School of Medicine, New York, NY) for the pEGFP-Rap1A-V12 and pEGFP-Rap1A-N17 plasmid constructs. We thank Life Magnetics for the nucleic acid isolation kits.

Conflict of interest

The authors declare that there are no conflicts of interest.

References

[1] Siegel R, Naishadham D, and Jemal A (2012). Cancer statistics, 2012. *CA Cancer J Clin* **62**, 10–29.
[2] Puliti D and Zappa M (2012). Breast cancer screening: are we seeing the benefit? *BMC Med* **10**, 106–109.
[3] Polyak K (2010). Molecular markers for the diagnosis and management of ductal carcinoma in situ. *J Natl Cancer Inst Monogr* **2010**, 210–213.
[4] Van Cleef A, Altintas S, Huizing M, Papadimitriou K, Van Dam P, and Tjalma W (2014). Current view on ductal carcinoma in situ and importance of the margin thresholds: A review. *Facts Views Vis Obgyn* **6**, 210–218.
[5] Kuerer HM, Albarracin CT, Yang WT, Cardiff RD, Brewster AM, Symmans WF, Hylton NM, Middleton LP, Krishnamurthy S, and Perkins GH, et al (2009). Ductal carcinoma in situ: state of the science and roadmap to advance the field. *J Clin Oncol* **27**, 279–288.
[6] Independent UKPoBCS (2012). The benefits and harms of breast cancer screening: an independent review. *Lancet* **380**, 1778–1786.
[7] Kaur H, Mao S, Shah S, Gorski DH, Krawetz SA, Sloane BF, and Mattingly RR (2013). Next-generation sequencing: a powerful tool for the discovery of molecular markers in breast ductal carcinoma in situ. *Expert Rev Mol Diagn* **13**, 151–165.
[8] Groen EJ, Elshof LE, Visser LL, Rutgers EJ, Winter-Warnars HA, Lips EH, and Wesseling J (2017). Finding the balance between over- and under-treatment of ductal carcinoma in situ (DCIS). *Breast* **31**, 274–283.
[9] Gotzsche PC and Nielsen M (2011). Screening for breast cancer with mammography. *Cochrane Database Syst Rev* CD001877.
[10] Gotzsche PC, Jorgensen KJ, Zahl PH, and Maehlen J (2012). Why mammography screening has not lived up to expectations from the randomised trials. *Cancer Causes Control* **23**, 15–21.
[11] Wang L, Hoque A, Luo RZ, Yuan J, Lu Z, Nishimoto A, Liu J, Sahin AA, Lippman SM, and Bast Jr RC, et al (2003). Loss of the expression of the tumor suppressor gene ARHI is associated with progression of breast cancer. *Clin Cancer Res* **9**, 3660–3666.
[12] Itoh M, Nelson CM, Myers CA, and Bissell MJ (2007). Rap1 integrates tissue polarity, lumen formation, and tumorigenic potential in human breast epithelial cells. *Cancer Res* **67**, 4759–4766.

[13] Furstenau DK, Mitra N, Wan F, Lewis R, Feldman MD, Fraker DL, and Guvakova MA (2011). Ras-related protein 1 and the insulin-like growth factor type I receptor are associated with risk of progression in patients diagnosed with carcinoma in situ. *Breast Cancer Res Treat* **129**, 361–372.

[14] Li W, Jin B, Cornelius LA, Zhou B, Fu X, Shang D, and Zheng H (2011). Inhibitory effects of Rap1GAP overexpression on proliferation and migration of endothelial cells via ERK and Akt pathways. *J Huazhong Univ Sci Technolog Med Sci* **31**, 721–727.

[15] Zheng H, Gao L, Feng Y, Yuan L, Zhao H, and Cornelius LA (2009). Down-regulation of Rap1GAP via promoter hypermethylation promotes melanoma cell proliferation, survival, and migration. *Cancer Res* **69**, 449–457.

[16] Zhang Z, Mitra RS, Henson BS, Datta NS, McCauley LK, Kumar P, Lee JS, Carey TE, and D'Silva NJ (2006). Rap1GAP inhibits tumor growth in oropharyngeal squamous cell carcinoma. *Am J Pathol* **168**, 585–596.

[17] Zhang L, Chenwei L, Mahmood R, van Golen K, Greenson J, Li G, D'Silva NJ, Li X, Burant CF, and Logsdon CD, et al (2006). Identification of a putative tumor suppressor gene Rap1GAP in pancreatic cancer. *Cancer Res* **66**, 898–906.

[18] Kim WJ, Gersey Z, and Daaka Y (2012). Rap1GAP regulates renal cell carcinoma invasion. *Cancer Lett* **320**, 65–71.

[19] Dong X, Tang W, Stopenski S, Brose MS, Korch C, and Meinkoth JL (2012). RAP1GAP inhibits cytoskeletal remodeling and motility in thyroid cancer cells. *Endocr Relat Cancer* **19**, 575–588.

[20] Miller FR, Soule HD, Tait L, Pauley RJ, Wolman SR, Dawson PJ, and Heppner GH (1993). Xenograft model of progressive human proliferative breast disease. *J Natl Cancer Inst* **85**, 1725–1732.

[21] Dawson PJ, Wolman SR, Tait L, Heppner GH, and Miller FR (1996). MCF10AT: a model for the evolution of cancer from proliferative breast disease. *Am J Pathol* **148**, 313–319.

[22] Miller FR, Santner SJ, Tait L, and Dawson PJ (2000). MCF10DCIS.com xenograft model of human comedo ductal carcinoma in situ. *J Natl Cancer Inst* **92**, 1185–1186.

[23] Santner SJ, Dawson PJ, Tait L, Soule HD, Eliason J, Mohamed AN, Wolman SR, Heppner GH, and Miller FR (2001). Malignant MCF10CA1 cell lines derived from premalignant human breast epithelial MCF10AT cells. *Breast Cancer Res Treat* **65**, 101–110.

[24] Osuala KO, Sameni M, Shah S, Aggarwal N, Simonait ML, Franco OE, Hong Y, Hayward SW, Behbod F, and Mattingly RR, et al (2015). Il-6 signaling between ductal carcinoma in situ cells and carcinoma-associated fibroblasts mediates tumor cell growth and migration. *BMC Cancer* **15**, 584–598.

[25] Li Q, Mullins SR, Sloane BF, and Mattingly RR (2008). p21-Activated kinase 1 coordinates aberrant cell survival and pericellular proteolysis in a three-dimensional culture model for premalignant progression of human breast cancer. *Neoplasia* **10**, 314–329.

[26] Li Q, Chow AB, and Mattingly RR (2010). Three-dimensional overlay culture models of human breast cancer reveal a critical sensitivity to mitogen-activated protein kinase kinase inhibitors. *J Pharmacol Exp Ther* **332**, 821–828.

[27] Li Q and Mattingly RR (2008). Restoration of E-cadherin cell-cell junctions requires both expression of E-cadherin and suppression of ERK MAP kinase activation in Ras-transformed breast epithelial cells. *Neoplasia* **10**, 1444–1458.

[28] Sameni M, Cavallo-Medved D, Franco OE, Chalasani A, Ji K, Aggarwal N, Anbalagan A, Chen X, Mattingly RR, and Hayward SW, et al (2017). Pathomimetic avatars reveal divergent roles of microenvironment in invasive transition of ductal carcinoma in situ. *Breast Cancer Res* **19**, 56–75.

[29] Tsygankova OM, Ma C, Tang W, Korch C, Feldman MD, Lv Y, Brose MS, and Meinkoth JL (2010). Downregulation of Rap1GAP in human tumor cells alters cell/matrix and cell/cell adhesion. *Mol Cell Biol* **30**, 3262–3274.

[30] Menard RE, Jovanovski AP, and Mattingly RR (2005). Active p21-activated kinase 1 rescues MCF10A breast epithelial cells from undergoing anoikis. *Neoplasia* **7**, 638–645.

[31] Kaur H, Mao S, Li Q, Sameni M, Krawetz SA, Sloane BF, and Mattingly RR (2012). RNA-Seq of human breast ductal carcinoma in situ models reveals aldehyde dehydrogenase isoform 5A1 as a novel potential target. *PLoS One* **7**e50249.

[32] Behbod F, Kittrell FS, LaMarca H, Edwards D, Kerbawy S, Heestand JC, Young E, Mukhopadhyay P, Yeh HW, and Allred DC, et al (2009). An intraductal human-in-mouse transplantation model mimics the subtypes of ductal carcinoma in situ. *Breast Cancer Res* **11**, R66.

[33] Rhee SS, Lim B, Kim HH, Wang Y, Aziz U, Butt U, Tang WX, Vuchak LA, DeMichele A, and Troxel AB, et al (2011). Rap1 GTPase activating protein (Rap1GAP) is downregulated in DCIS and invasive ductal carcinoma. *Cancer Res* **71**.

[34] Ethier SP (1996). Human breast cancer cell lines as models of growth regulation and disease progression. *J Mammary Gland Biol Neoplasia* **1**, 111–121.

[35] Ethier SP, Mahacek ML, Gullick WJ, Frank TS, and Weber BL (1993). Differential isolation of normal luminal mammary epithelial cells and breast cancer cells from primary and metastatic sites using selective media. *Cancer Res* **53**, 627–635.

[36] Subik K, Lee JF, Baxter L, Strzepek T, Costello D, Crowley P, Xing L, Hung MC, Bonfiglio T, and Hicks DG, et al (2010). The expression patterns of ER, PR, HER2, CK5/6, EGFR, Ki-67 and AR by immunohistochemical analysis in breast cancer cell lines. *Breast Cancer* **4**, 35–41.

[37] Holliday DL and Speirs V (2011). Choosing the right cell line for breast cancer research. *Breast Cancer Res* **13**, 215–222.

[38] Neve RM, Chin K, Fridlyand J, Yeh J, Baehner FL, Fevr T, Clark L, Bayani N, Coppe JP, and Tong F, et al (2006). A collection of breast cancer cell lines for the study of functionally distinct cancer subtypes. *Cancer Cell* **10**, 515–527.

[39] Grigoriadis A, Mackay A, Noel E, Wu PJ, Natrajan R, Frankum J, Reis-Filho JS, and Tutt A (2012). Molecular characterisation of cell line models for triple-negative breast cancers. *BMC Genomics* **13**, 619–633.

[40] Lombaerts M, van Wezel T, Philippo K, Dierssen JW, Zimmerman RM, Oosting J, van Eijk R, Eilers PH, van de Water B, and Cornelisse CJ, et al (2006). E-cadherin transcriptional downregulation by promoter methylation but not mutation is related to epithelial-to-mesenchymal transition in breast cancer cell lines. *Br J Cancer* **94**, 661–671.

[41] Graff JR, Gabrielson E, Fujii H, Baylin SB, and Herman JG (2000). Methylation patterns of the E-cadherin 5' CpG island are unstable and reflect the dynamic, heterogeneous loss of E-cadherin expression during metastatic progression. *J Biol Chem* **275**, 2727–2732.

[42] Chao YL, Shepard CR, and Wells A (2010). Breast carcinoma cells re-express E-cadherin during mesenchymal to epithelial reverting transition. *Mol Cancer* **9**, 179–197.

[43] Hollestelle A, Peeters JK, Smid M, Timmermans M, Verhoog LC, Westenend PJ, Heine AA, Chan A, Sieuwerts AM, and Wiemer EA, et al (2013). Loss of E-cadherin is not a necessity for epithelial to mesenchymal transition in human breast cancer. *Breast Cancer Res Treat* **138**, 47–57.

[44] Yamaguchi H and Condeelis J (2007). Regulation of the actin cytoskeleton in cancer cell migration and invasion. *Biochim Biophys Acta* **1773**, 642–652.

[45] Mouneimne G, Hansen SD, Selfors LM, Petrak L, Hickey MM, Gallegos LL, Simpson KJ, Lim J, Gertler FB, and Hartwig JH, et al (2012). Differential remodeling of actin cytoskeleton architecture by profilin isoforms leads to distinct effects on cell migration and invasion. *Cancer Cell* **22**, 615–630.

[46] Park S, Jung HH, Park YH, Ahn JS, and Im YH (2011). ERK/MAPK pathways play critical roles in EGFR ligands-induced MMP1 expression. *Biochem Biophys Res Commun* **407**, 680–686.

[47] Ma L, Lan F, Zheng Z, Xie F, Wang L, Liu W, Han J, Zheng F, Xie Y, and Huang Q (2012). Epidermal growth factor (EGF) and interleukin (IL)-1beta synergistically promote ERK1/2-mediated invasive breast ductal cancer cell migration and invasion. *Mol Cancer* **11**, 79–90.

[48] Tsygankova OM, Feshchenko E, Klein PS, and Meinkoth JL (2004). Thyroid-stimulating hormone/cAMP and glycogen synthase kinase 3beta elicit opposing effects on Rap1GAP stability. *J Biol Chem* **279**, 5501–5507.

[49] Livasy CA, Perou CM, Karaca G, Cowan DW, Maia D, Jackson S, Tse CK, Nyante S, and Millikan RC (2007). Identification of a basal-like subtype of breast ductal carcinoma in situ. *Hum Pathol* **38**, 197–204.

[50] Clark SE, Warwick J, Carpenter R, Bowen RL, Duffy SW, and Jones JL (2011). Molecular subtyping of DCIS: heterogeneity of breast cancer reflected in pre-invasive disease. *Br J Cancer* **104**, 120–127.

[51] Lesurf R, Aure MR, Mork HH, Vitelli V, Oslo Breast Cancer Research CLundgren S, Borresen-Dale AL, Kristensen V, Warnberg F, and Hallett M, et al (2016). Molecular features of subtype-specific progression from ductal carcinoma in situ to invasive breast cancer. *Cell Rep* **16**, 1166–1179.

[52] Lehmann BD, Bauer JA, Chen X, Sanders ME, Chakravarthy AB, Shyr Y, and Pietenpol JA (2011). Identification of human triple-negative breast cancer subtypes and preclinical models for selection of targeted therapies. *J Clin Invest* **121**, 2750–2767.

[53] Jezequel P, Loussouarn D, Guerin-Charbonnel C, Campion L, Vanier A, Gouraud W, Lasla H, Guette C, Valo I, and Verriele V, et al (2015). Gene-expression molecular subtyping of triple-negative breast cancer tumours: importance of immune response. *Breast Cancer Res* **17**, 43–59.

[54] Burstein MD, Tsimelzon A, Poage GM, Covington KR, Contreras A, Fuqua SA, Savage MI, Osborne CK, Hilsenbeck SG, and Chang JC, et al (2015). Comprehensive genomic analysis identifies novel subtypes and targets of triple-negative breast cancer. *Clin Cancer Res* **21**, 1688–1698.
[55] Kumar P and Aggarwal R (2016). An overview of triple-negative breast cancer. *Arch Gynecol Obstet* **293**, 247–269.
[56] Ahn SG, Kim SJ, Kim C, and Jeong J (2016). Molecular classification of triple-negative breast cancer. *J Breast Cancer* **19**, 223–230.
[57] Kenny PA, Lee GY, Myers CA, Neve RM, Semeiks JR, Spellman PT, Lorenz K, Lee EH, Barcellos-Hoff MH, and Petersen OW, et al (2007). The morphologies of breast cancer cell lines in three-dimensional assays correlate with their profiles of gene expression. *Mol Oncol* **1**, 84–96.
[58] Sproul D, Nestor C, Culley J, Dickson JH, Dixon JM, Harrison DJ, Meehan RR, Sims AH, and Ramsahoye BH (2011). Transcriptionally repressed genes become aberrantly methylated and distinguish tumors of different lineages in breast cancer. *Proc Natl Acad Sci U S A* **108**, 4364–4369.
[59] Prat A, Parker JS, Karginova O, Fan C, Livasy C, Herschkowitz JI, He X, and Perou CM (2010). Phenotypic and molecular characterization of the claudin-low intrinsic subtype of breast cancer. *Breast Cancer Res* **12**R68.
[60] Alemayehu M, Dragan M, Pape C, Siddiqui I, Sacks DB, Di Guglielmo GM, Babwah AV, and Bhattacharya M (2013). beta-Arrestin2 regulates lysophosphatidic acid-induced human breast tumor cell migration and invasion via Rap1 and IQGAP1. *PLoS One* **8**e56174.
[61] Tsygankova OM, Wang H, and Meinkoth JL (2013). Tumor cell migration and invasion are enhanced by depletion of Rap1 GTPase-activating protein (Rap1GAP). *J Biol Chem* **288**, 24636–24646.
[62] De Craene B and Berx G (2013). Regulatory networks defining EMT during cancer initiation and progression. *Nat Rev Cancer* **13**, 97–110.
[63] Thompson EW, Torri J, Sabol M, Sommers CL, Byers S, Valverius EM, Martin GR, Lippman ME, Stampfer MR, and Dickson RB (1994). Oncogene-induced basement membrane invasiveness in human mammary epithelial cells. *Clin Exp Metastasis* **12**, 181–194.
[64] Hogan C, Serpente N, Cogram P, Hosking CR, Bialucha CU, Feller SM, Braga VM, Birchmeier W, and Fujita Y (2004). Rap1 regulates the formation of E-cadherin-based cell-cell contacts. *Mol Cell Biol* **24**, 6690–6700.
[65] Balzac F, Avolio M, Degani S, Kaverina I, Torti M, Silengo L, Small JV, and Retta SF (2005). E-cadherin endocytosis regulates the activity of Rap1: a traffic light GTPase at the crossroads between cadherin and integrin function. *J Cell Sci* **118**, 4765–4783.
[66] Asuri S, Yan J, Paranavitana NC, and Quilliam LA (2008). E-cadherin disengagement activates the Rap1 GTPase. *J Cell Biochem* **105**, 1027–1037.
[67] Yang Y, Zhang J, Yan Y, Cai H, Li M, Sun K, Wang J, Liu X, Wang J, and Duan X (2017). Low expression of Rap1GAP is associated with epithelial-mesenchymal transition (EMT) and poor prognosis in gastric cancer. *Oncotarget* **8**, 8057–8068.
[68] Zuo H, Gandhi M, Edreira MM, Hochbaum D, Nimgaonkar VL, Zhang P, Dipaola J, Evdokimova V, Altschuler DL, and Nikiforov YE (2010). Downregulation of Rap1GAP through epigenetic silencing and loss of heterozygosity promotes invasion and progression of thyroid tumors. *Cancer Res* **70**, 1389–1397.
[69] Tamate M, Tanaka R, Osogami H, Matsuura M, Satohisa S, Iwasaki M, and Saito T (2017). Rap1GAP inhibits tumor progression in endometrial cancer. *Biochem Biophys Res Commun* **485**, 476–483.
[70] Wu K, Jerdeva GV, da Costa SR, Sou E, Schechter JE, and Hamm-Alvarez SF (2006). Molecular mechanisms of lacrimal acinar secretory vesicle exocytosis. *Exp Eye Res* **83**, 84–96.
[71] Lamouille S, Xu J, and Derynck R (2014). Molecular mechanisms of epithelial-mesenchymal transition. *Nat Rev Mol Cell Biol* **15**, 178–196.
[72] Schwamborn JC and Puschel AW (2004). The sequential activity of the GTPases Rap1B and Cdc42 determines neuronal polarity. *Nat Neurosci* **7**, 923–929.
[73] Bos JL (2005). Linking Rap to cell adhesion. *Curr Opin Cell Biol* **17**, 123–128.
[74] Lu L, Wang J, Wu Y, Wan P, and Yang G (2016). Rap1A promotes ovarian cancer metastasis via activation of ERK/p38 and notch signaling. *Cancer Med* **5**, 3544–3554.
[75] Shah S, Brock EJ, Ji K, and Mattingly RR (2018). Ras and Rap1: a tale of two GTPases. *Semin Cancer Biol* In press.
[76] Wu J-X, Du W-Q, Wang X-C, Wei L-L, Huo F-C, Pan Y-J, Wu X-J, and Pei D-S (2017). Rap2a serves as a potential prognostic indicator of renal cell carcinoma and promotes its migration and invasion through up-regulating p-Akt. *Sci Rep* **7**, 6623–6634.
[77] Tsygankova OM, Prendergast GV, Puttaswamy K, Wang Y, Feldman MD, Wang H, Brose MS, and Meinkoth JL (2007). Downregulation of Rap1GAP contributes to Ras transformation. *Mol Cell Biol* **27**, 6647–6658.
[78] Weinberg RA (1991). Tumor suppressor genes. *Science* **254**, 1138–1146.
[79] Qiu T, Qi X, Cen J, and Chen Z (2012). Rap1GAP alters leukemia cell differentiation, apoptosis and invasion in vitro. *Oncol Rep* **28**, 622–628.
[80] Wang D, Zhang P, Gao K, Tang Y, Jin X, Zhang Y, Yi Q, Wang C, and Yu L (2014). PLK1 and beta-TrCP-dependent ubiquitination and degradation of Rap1GAP controls cell proliferation. *PLoS One* **9**e110296.
[81] Nellore A, Paziana K, Ma C, Tsygankova OM, Wang Y, Puttaswamy K, Iqbal AU, Franks SR, Lv Y, and Troxel AB, et al (2009). Loss of Rap1GAP in papillary thyroid cancer. *J Clin Endocrinol Metab* **94**, 1026–1032.
[82] Bailey CL, Kelly P, and Casey PJ (2009). Activation of Rap1 promotes prostate cancer metastasis. *Cancer Res* **69**, 4962–4968.
[83] Li L, Wang S, Jezierski A, Moalim-Nour L, Mohib K, Parks RJ, Retta SF, and Wang L (2010). A unique interplay between Rap1 and E-cadherin in the endocytic pathway regulates self-renewal of human embryonic stem cells. *Stem Cells* **28**, 247–257.
[84] Hynes RO (2002). Integrins: bidirectional, allosteric signaling machines. *Cell* **110**, 673–687.
[85] Post A, Pannekoek WJ, Ross SH, Verlaan I, Brouwer PM, and Bos JL (2013). Rasip1 mediates Rap1 regulation of Rho in endothelial barrier function through ArhGAP29. *Proc Natl Acad Sci U S A* **110**, 11427–11432.
[86] Hsieh SM, Smith RA, Lintell NA, Hunter KW, and Griffiths LR (2009). Polymorphisms of the SIPA1 gene and sporadic breast cancer susceptibility. *BMC Cancer* **9**, 331–337.
[87] Yi SM and Li GY (2014). The association of SIPA1 gene polymorphisms with breast cancer risk: evidence from published studies. *Tumour Biol* **35**, 441–445.
[88] Crawford NP, Ziogas A, Peel DJ, Hess J, Anton-Culver H, and Hunter KW (2006). Germline polymorphisms in SIPA1 are associated with metastasis and other indicators of poor prognosis in breast cancer. *Breast Cancer Res* **8**R16.
[89] Gaudet MM, Hunter K, Pharoah P, Dunning AM, Driver K, Lissowska J, Sherman M, Peplonska B, Brinton LA, and Chanock S, et al (2009). Genetic variation in SIPA1 in relation to breast cancer risk and survival after breast cancer diagnosis. *Int J Cancer* **124**, 1716–1720.
[90] Zhang Y, Gong Y, Hu D, Zhu P, Wang N, Zhang Q, Wang M, Aldeewan A, Xia H, and Qu X, et al (2015). Nuclear SIPA1 activates integrin beta1 promoter and promotes invasion of breast cancer cells. *Oncogene* **34**, 1451–1462.